processes

MDPI

Article

Optimal Pathways for Nitric Acid Synthesis Using P-Graph Attainable Region Technique (PART)

Yiann Sitoh [1], Viggy Wee Gee Tan [1], John Frederick D. Tapia [2], Raymond R. Tan [2] and Dominic C. Y. Foo [1,*]

[1] Department of Chemical and Environmental Engineering, University of Nottingham Malaysia, Broga Road, Semenyih 43500, Malaysia; sitohyiann@gmail.com (Y.S.); vgweegee@gmail.com (V.W.G.T.)
[2] Department of Chemical Engineering, De La Salle University, 2401 Taft Avenue, Malate, Manila 0922, Philippines; john.frederick.tapia@dlsu.edu.ph (J.F.D.T.); raymond.tan@dlsu.edu.ph (R.R.T.)
* Correspondence: dominic.foo@nottingham.edu.my

Abstract: Developing a chemical reaction network is considered the first and most crucial step of process synthesis. Many methods have been employed for process synthesis, such as the attainable region (AR) theory. AR states that a region of all possible configurations can be defined with all the potential products and reactants. The second method is process network synthesis (PNS), a technique used to optimise a flowsheet based on the feasible materials and energy flow. P-graph is an algorithmic framework for PNS problems. P-graph attainable region technique (PART) is introduced here as an integration of both AR and P-graph to generate optimal reaction pathways for a given process. A descriptive AR plot is also developed to represent all the possible solution structures or reaction pathways. A case study of a conventional nitric acid synthesis process was used to demonstrate this technique.

Keywords: attainable region; process network synthesis; chemical reaction network; P-graph; nitric acid synthesis

Citation: Sitoh, Y.; Tan, V.W.G.; Tapia, J.F.D.; Tan, R.R.; Foo, D.C.Y. Optimal Pathways for Nitric Acid Synthesis Using P-Graph Attainable Region Technique (PART). *Processes* **2023**, *11*, 2684. https://doi.org/10.3390/pr11092684

Academic Editors: Thomas S.Y. Choong and Hazlina Husin

Received: 26 June 2023
Revised: 22 August 2023
Accepted: 23 August 2023
Published: 7 September 2023

1. Introduction

Process synthesis is a critical aspect of chemical engineering that involves creating and designing new processes for producing chemicals and materials [1]. It is a multidisciplinary field that brings together concepts from chemistry, biology, biochemistry, computer science, and materials to create efficient and sustainable manufacturing processes [2]. The process synthesis approach involves identifying the key process variables, analysing the available feedstock and energy sources, and designing the optimal process flowsheet to achieve the desired product quality and quantity [3]. The ultimate goal of process synthesis is to develop economically viable and environmentally sustainable processes that can be implemented at an industrial scale [4]. At the core of process synthesis, making decision on chemical reaction is the first and most crucial step, as it will dictate decision to be made on other parts of the process [5].

In the past few decades, different approaches have been reported to ease the development of process reaction pathways and process synthesis. Among them, the *attainable region* (AR) and *process network synthesis* (PNS) are among two known approaches that are widely used to synthesise reaction pathways and process synthesis. AR was first introduced by Horn [6] in chemical reaction engineering, where he defined it as the region of all possible products and configurations with various kinetics and feed regimes. The chemical process usually consists of reactions with intrinsic heat and mass transfer effects [7]. AR utilised such properties of the process to generate a geometrical region to represent all possible outcomes derived from a combination of parameters bound by lines showing the limitations of the system [8]. Input variables into the process, such as material flowrates, energy flowrates, etc., are important to be optimised to ensure high resource efficiency. This allows the search for specific desirable objectives from a reaction system either to maximise

product selectivity or minimise cost and emissions. Over the years, the AR technique has been used extensively to aid process synthesis. An earlier example of the application of AR has been studied by Mcgregor et al. [9] on a reactor–separator–recycle system. Another work by Hildebrandt et al. [10] showed that the geometric AR approach can be used to derive sets of new conditions for a system of known reactions, which allows them to obtain new configurations of several reactor systems. In another work by Nicol et al. [11], the use of AR has been extended to find optimum process designs while incorporating the cost of utilities. The inclusion of utility cost introduces a new complexity to the application of AR. Apart from using AR for process synthesis, AR theory can also be applied to process debottlenecking. This was demonstrated by Moodley et al. [12] who successfully investigated the limitation of an ammonia synthesis reactor system; the latter has a low degree of freedom and can be difficult to modify. In more recent years, the application of AR can be seen in newer processes. One of these examples is the production of bioethanol from lignocellulose. Though this semi-commercial process is able to produce bioethanol from unwanted biomass, it still requires optimisation and improvement to achieve economic success [13]. With this in mind, some researchers have employed AR techniques to analyse and improve the effectiveness of the bioreactor configuration to boost the production of bioethanol [14].

Yet another important method for process synthesis method is PNS, which is a method used to optimise material and energy flows in finding combinatorically feasible structures for specific systems [15]. The process graph (P-graph) framework is a family of algorithms used for solving the PNS problem [16]. The algorithms are rigorously developed from a set of axioms for PNS problems [17]. These component algorithms are maximal structure generation (MSG) [17], solution structure generation [18], and maximal structure generation [19]. The software tool P-graph Studio v5.2.4.4 provides a user-friendly implementation of this computing framework [20]. The P-graph framework is efficient in solving problems with high combinatorial complexity and shows great ability in reducing computational workload [21]. P-graph can be applied to developing a cost-effective flowsheet for downstream biochemical processing [22]. The procedure starts with the inclusion of all possible processing units, followed by the generation of optimal solution structures. A unique optimization model can be generated for each of these structures. The solutions can be used by engineers for future process selection.

After years of development, P-graph is no longer limited to solving PNS problems. The extension of P-graph on carbon management network [23], as well as carbon capture and storage [24] have also been reported. Besides, Lim et al. [25] extended P-graph methodology for material resource conservation. As mentioned, the generation of a reaction equation is crucial for process synthesis. The ability of the P-graph to identify and generate biochemical reactions and metabolic pathways has been reported [26]. Similarly, Fan et al. [27] have also investigated the potential of process synthesis for the synthesis of candidate pathways or the mechanism of a catalytic reaction. An additional variant for determining startable chemical reaction networks has been studied [28].

Though AR and P-graph both find their application in process synthesis, there are limited studies on the integration of both techniques. The *P-graph attainable region technique* (PART) was recently introduced as a way to generate an optimal reaction pathway for a given process [24]. This seminal work demonstrated PART as an effective approach for the construction of reaction equations for a chemical process.

This study addresses this research gap by extending the PART through the introduction of an AR plot to improve the interpretability of the solution set. The AR plot consists of all feasible solutions within the defined region, which allows designers to better scrutinise the different configurations of a synthesis problem. An example of nitric acid synthesis will be employed to demonstrate this approach, and each solution structure will be analysed and converted into a process block diagram.

2. Methodology

P-graphs are bipartite graphs, each comprising nodes for a set of materials (M-type), a set of operating units (O-type), and arcs linking them [29]. M-type nodes can be further divided into raw material, intermediate material, and product material nodes. Figure 1 is an example adapted from Pimentel et al. [30] used to illustrate the types of nodes in P-graph. This diagram represents a vapour generation process using biomass and purified water in a boiler. The boiler is represented by the O-type nodes, while purified water, biomass, and steam are represented by M-type nodes.

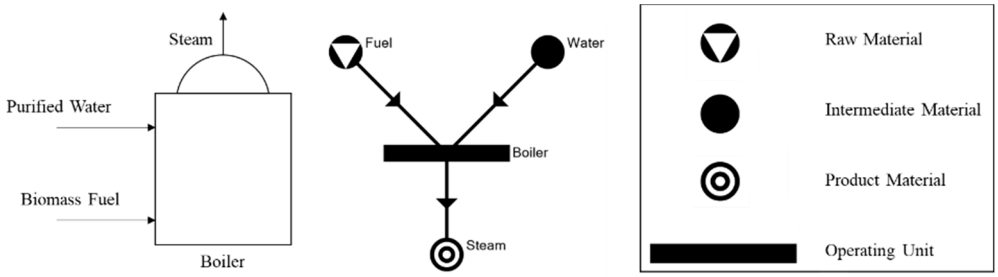

Figure 1. P-graph configuration example [30].

P-graph Studio is used here to implement the MSG, SSG, and ABB algorithms [20]. In this study, the optimal solution structure will be generated with the ABB algorithm using the procedure adapted from Bertok and Heckl [29] and Tapia et al. [31].

The procedure for using P-Graph technique is as follows:

1. There are five types of nodes in the process, namely, reactant, product, element, energy, and material inlet/outlet.
2. Each chemical component is either represented by a reactant, product node, or both. When the structures are generated, the node representing the chemical component will be either a reactant or product node only.
3. Reactants are represented by the raw material node; products are represented by the product material node; and Gibbs energy, enthalpy, and element are represented by the intermediate node. The chemical components are also represented as operating unit nodes with one node for each role in the process (i.e., product or reactant).
4. Each reactant will be connected to a material input node, where the outputs will be connected to an element node based on the element constituent of the reactant (e.g., in the case of CH_4, the reactant will be connected to C and H element nodes while specifying the C unit flow rate to 1, and that of H to 4).
5. The flow required for each of the element nodes is based on the system balance of producing 1 mole of nitric acid. Therefore, the flow requirement will be 1 for H and N nodes and 3 for the O node.
6. Node and flow of each component are represented by its own unique colour.
7. Other side products are connected to the output unit, where the input is connected to the element node based on the element constituent of the products.
8. The heat of formation and Gibbs energy of a reactant/product will also be connected to the respective energy node while specifying the energy value on the unit flow rate to represent the system's energy balance.
9. A positive value of energy will be connected on a forward flow, while a negative value of energy will be connected as a backward flow (e.g., in the case of CH_4, the flow rate to Gibbs energy node will be -74 kJ/mol, resulting in a backward configuration with a flowrate of 74).

Next, the AR plot will be produced using the procedure developed by Patel et al. [8] as the foundation. In his work, AR plot is produced based on linear mathematical mass balance equations. This method is excellent in solving systems with low degree of freedom (DOF). More complex mathematical methods are required for system with two or more DOF. In this study, results from P-graph will be used to construct AR plot instead of using

mathematical approach. Additionally, estimated production cost will be plotted on a secondary axis to provide more insight into the process.

The procedure for using PART technique is as follows:

1. The AR plot is constructed based on the production of 1 mol of the desired product (e.g., consider a reaction $3A + B = 2C + 3D$; if C is the main product, the equation will be simplified to $1.5A + 0.5B = C + 1.5D$).
2. *X*-axis of the plot represents the moles input of the main reactant.
3. Positive region of *Y*-axis represents the moles input of other process components, while negative region represents that of the output of other process components (e.g., consider $1.5A + 0.5B = C + 1.5D$; component A and B will be plotted on the positive region while component D will be plotted on the negative region).
4. Each of the points of the component line will be plotted based on each of the P-graph solutions. Figure 2 shows the example plot of 3 solutions.

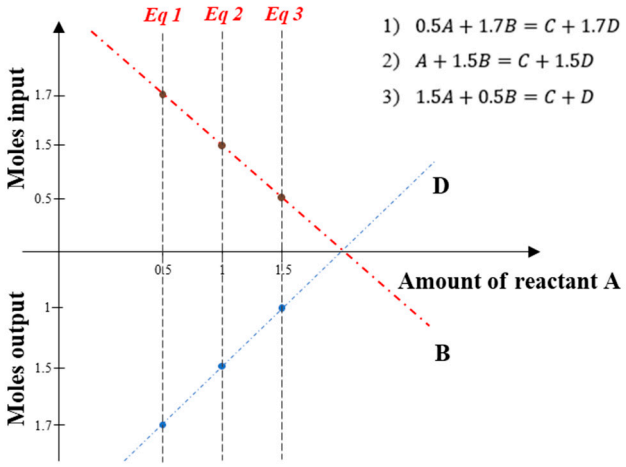

Figure 2. Attainable region plot example.

5. Extrapolating the component line expands the range of possible solutions for the system.
6. Production cost, USD/moles of the main product produced, will be plotted on a secondary axis against the moles input of the main reactant.
7. The gross production cost will be calculated with Equation (1).

$$\text{Gross Production cost} = \sum \text{Cost of Reactant} \quad (1)$$

3. Case Study: Nitric Acid Synthesis

The synthesis of nitric acid will be used as a case study to demonstrate the approach of extended PART. Commercially, nitric acid is synthesised using the Ostwald process, which involves the oxidation of ammonia [32]. Three main stages are involved in the Ostwald process. The first stage is the oxidation of ammonia (NH_3) to produce nitric acid (NO) and water (H_2O). The second step is the formation of nitrogen dioxide (NO_2) via the oxidation of NO. The final stage is the formation of nitric acid from NO_2 and H_2O along with NO as by-products. The equation of each stage of the Ostwald process is represented by Equations (2)–(4). Figure 3 shows the process flow diagram for a conventional Ostwald process.

$$4NH_3 + 5O_2 \rightarrow 4NO + 6H_2O \quad (2)$$

$$2NO + O_2 \rightarrow 2NO_2 \quad (3)$$

$$3NO_2 + H_2O \rightarrow 2HNO_3 + NO \quad (4)$$

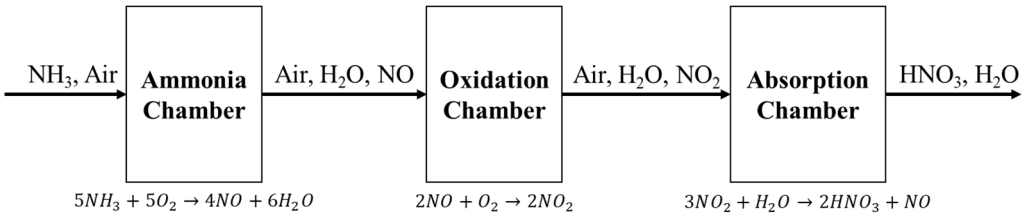

Figure 3. Process flow diagram for a conventional Ostwald process [33].

The possible inputs involved in the synthesis of one mole of Nitric acid (HNO_3) are NO_2, NO, O_2, and H_2O, with NH_3 being the main reactant. All these components are assumed to be in gaseous form and can be represented with Equation (5).

$$aNO_2(g) + bO_2(g) + cH_2O(l) + dNO(g) + eNH_3(g) \rightarrow HNO_3 \quad (5)$$

where a, b, c, d, e is the equation stoichiometry for each component to produce one mole of nitric acid. These components are selected just to demonstrate the approach, in which one can select different desired chemical components based on their respective process configurations. The heat of the reaction, ΔH_{rxn}, and the standard Gibbs energy, ΔG_{rxn}, can be represented by Equations (6) and (7).

$$\Delta H_{rxn} = \Delta H_{HNO_3} - a\Delta H_{NO_2} - b\Delta H_{O_2} - c\Delta H_{H_2O} - d\Delta H_{NO} - e\Delta H_{NH_3} \quad (6)$$

$$\Delta G_{rxn} = \Delta G_{HNO_3} - a\Delta G_{NO_2} - b\Delta G_{O_2} - c\Delta G_{H_2O} - d\Delta G_{NO} - e\Delta G_{NH_3} \quad (7)$$

where ΔH_i is the enthalpy and ΔG_i is the standard Gibbs energy of each component of the system, i. Table 1 shows the standard enthalpies at 298 K and 1 atm.

Table 1. Standard enthalpies and Gibbs energy of formation of involving component [34,35].

Chemical Component	Standard Heat of Formation (ΔH, kJ/mol)	Standard Gibbs Energy of Formation (ΔG, kJ/mol)
NO_2	33.18	−38.43
NO	90.25	−27.48
H_2O	−241.82	−228.57
O_2	0	0
NH_3	46.00	−16.50
HNO_3	−206.28	−79.91

The P-graph results are generated in the initial step of PART. Figure 4 shows the maximal structure for the case study, which is the union of all combinatorically feasible process structures of this case study [36]. This study is based on the production of one mole of nitric acid, where the element balance constraint for the system will be one mol of H, one mol of N and three mol of O. This ensures the production of one mol of nitric acid for all the solutions. The second constraint for the system will be based on ΔH and ΔG of the product. In this case, the required flow for both enthalpy and the Gibbs node will be −206.28 kJ/mol and −79.91 kJ/mol, respectively, which corresponds to that of nitric acid. Each of the components is connected to two nodes, "component in" nodes as the consumption nodes and "component out" nodes as the generation nodes.

The optimal solution for the study is the generated ABB algorithm, where the other partial problems are reduced and minimised [37]. Three out of five solution structures that involve NH_3 as a reactant are selected for analysis.

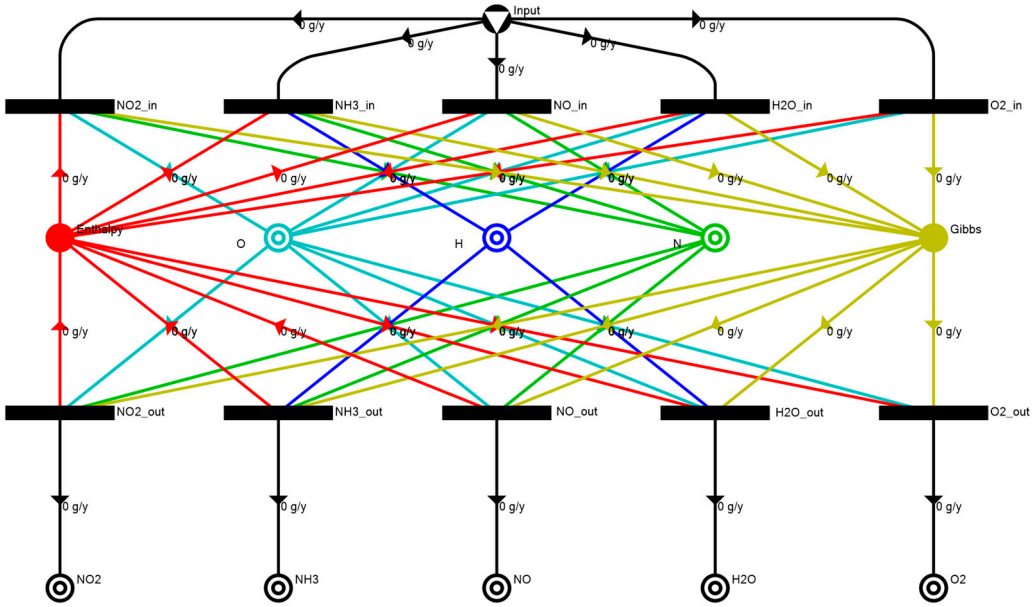

Figure 4. Nitric acid synthesis maximal solution structure.

The first solution (Figure 5) describes the production of nitric acid from NH_3 and NO_2 with NO as by-products. By evaluating the flowrate of each line, reaction equation and energy can be obtained. This reaction is exothermic and has a negative work requirement of −111.5 kJ, meaning that the reaction is spontaneous. The reaction equation is shown in Equation (8).

$$\begin{gathered} 2.33NO_2 + 0.33NH_3 \rightarrow HNO_3 + 1.67NO \\ \Delta H = -148.65kJ, \Delta G = -30.82kJ \end{gathered} \quad (8)$$

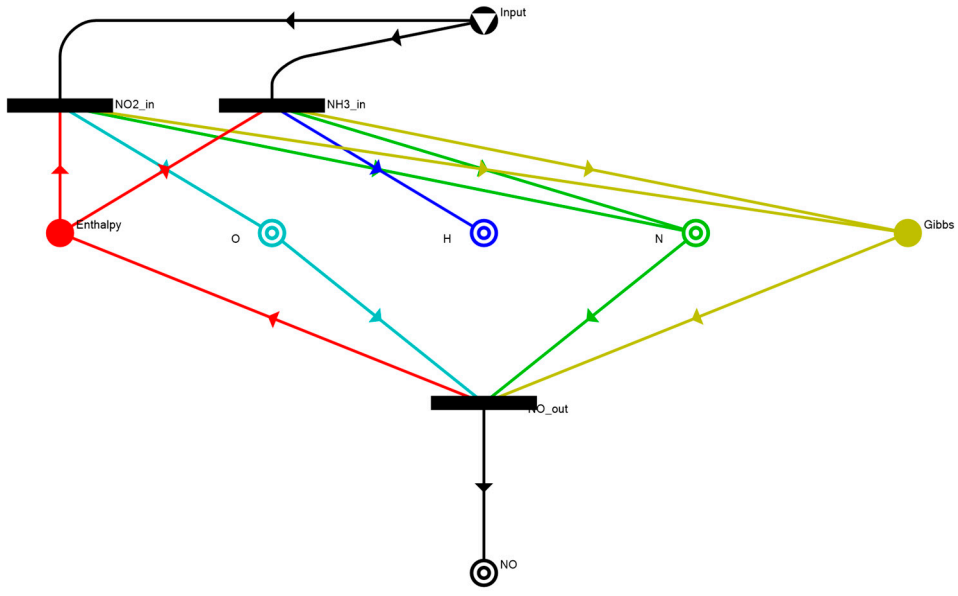

Figure 5. Nitric acid synthesis solution structure 1.

Figure 6 shows the block diagram representation of solution structure 1. It can be seen that this solution does not require any oxygen input like the usual Ostwald process. Instead, NO_2 is decomposed to produce oxygen along with NO as a by-product. The produced oxygen will be used to oxidise NH_3 to produce H_2O and NO. NO will be removed as by-products, while H_2O produced will be used for the formation of nitric acid. During this stage, additional NO_2 will be fed to aid the formation of nitric acid. This solution shows the possibility for nitric acid generation if oxygen is not a readily available raw material.

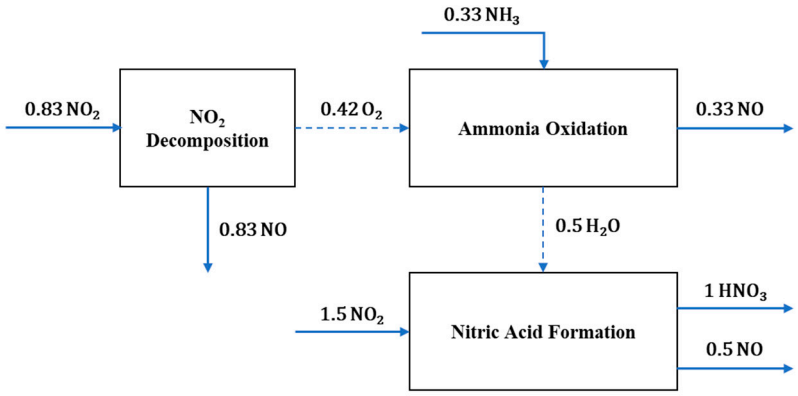

Figure 6. Process block diagram for solution structure 1.

Figure 7 shows the second solution structure of nitric acid synthesis. The second structure is similar to the first solution structure. This solution reduces the NO_2 feed into the system while requiring additional H_2O during the nitric acid formation stage. This could possibly reduce the cost of the process as H_2O is cheap and readily available in most situations. Besides reducing the cost of production, this solution also reduces the NO by-product formation. The overall process is represented in Figure 8. The reaction equation is shown in Equation (9).

$$2.1NO_2 + 0.14H_2O + 0.24NH_3 \rightarrow HNO_3 + 1.34NO$$
$$\Delta H = -132.168\text{kJ}, \Delta G = 0\text{kJ} \quad (9)$$

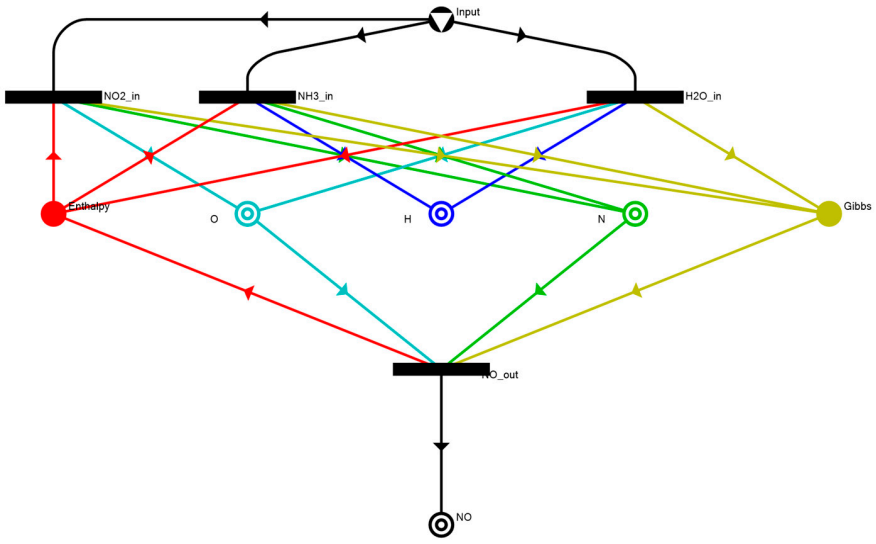

Figure 7. Nitric acid synthesis solution structure 2.

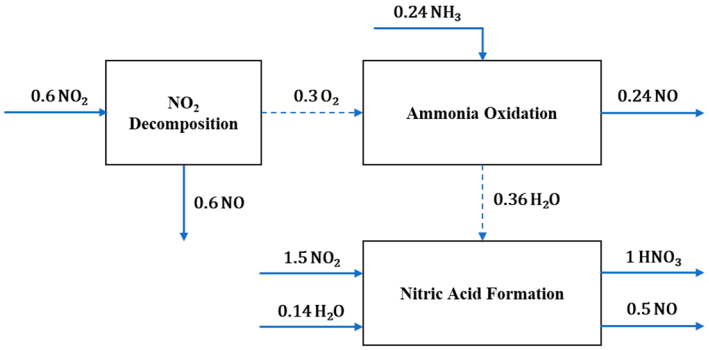

Figure 8. Process block diagram for solution structure 2.

The third solution structure is shown in Figure 9 and can be represented by Equation (10). In this solution, NO, H_2O, O_2 and NH_3 are used as feed to produce nitric acid. The work requirement of this solution is 0, indicating that the reaction is in equilibrium.

$$0.83NO + 0.24H_2O + 0.9685O_2 + 0.175NH_3 \rightarrow HNO_3$$
$$\Delta H = -231.294kJ, \Delta G = 0kJ \quad (10)$$

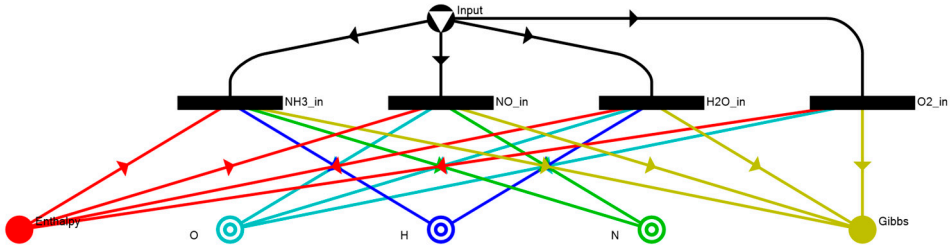

Figure 9. Nitric acid synthesis solution structure 3.

This solution provides a more interesting and complex insight into the process. As seen in Figure 9, this solution does not produce any by-products. This is essentially impossible as the elementary reaction of nitric acid formation will always produce NO as by-products, as shown in Equation (4). The absence of by-products can be interpreted as the full utilisation of NO with a recycle stream. The first stage of this solution shows the oxidation of NH_3, followed by the oxidation of NO. The NO produced along the formation of nitric acid will also be re-fed into this stage to eliminate any by-products. The block diagram of solution structure three represents a recycling loop (Figure 10).

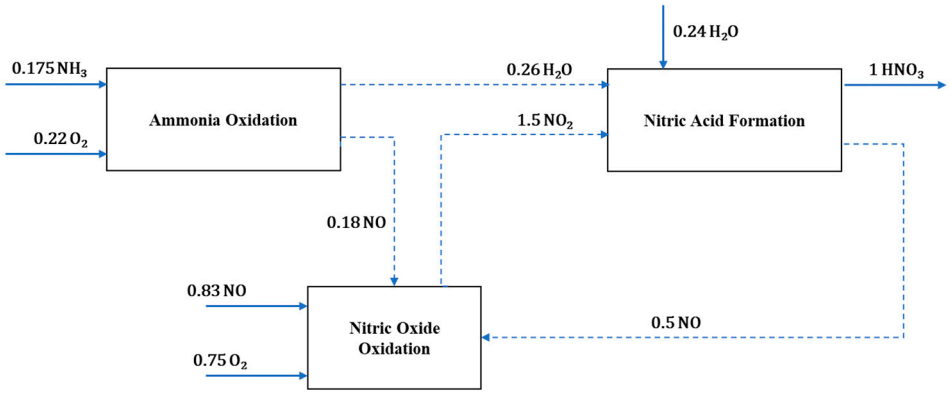

Figure 10. Process block diagram for solution structure 3.

The results above prove that the solution generated by the P-graph is not limited to conventional solutions. More complex solutions, such as those that involve recycling, can also be identified. This would provide useful insight for users to re-configure an existing setup while maintaining the validity of the new system with the use of constraints.

The next phase is the generation of the AR plot. By combining the solution structure obtained previously, an AR plot can be produced to illustrate the number of components required or produced as a function of feed. In this case, the AR graph will be plotted as the function of the amount of ammonia fed. Table 2 shows the summarised P-graph solution used to create the AR plot.

This is a meaningful plot as it can be used to select processes where there are certain constraints on the materials used/produced. For example, one can select a process that consumes NO in the region lying to the left of line A or a process that produces NO that lies to the right of point A. As shown in Figure 11, the region that lies left to line A essentially means a NO recycling system as it requires the least amount of NO_2 feed. If NO is not recycled, additional NO_2 is required to be fed into the system to achieve the desired conversion, which corresponds to the right region of line A.

Table 2. Stoichiometry of each compound for respective solution structure.

Solution	Chemical Compound						
	NH_3	NO_2	NO	H_2O	O_2	E	G
1	0.33	2.33	−1.67	0	0	−148.65	−30.54
2	0.24	2.1	−1.34	0.14	0	−132.20	0
3	0.175	0	0.83	0.237	0.9685	−231.92	0

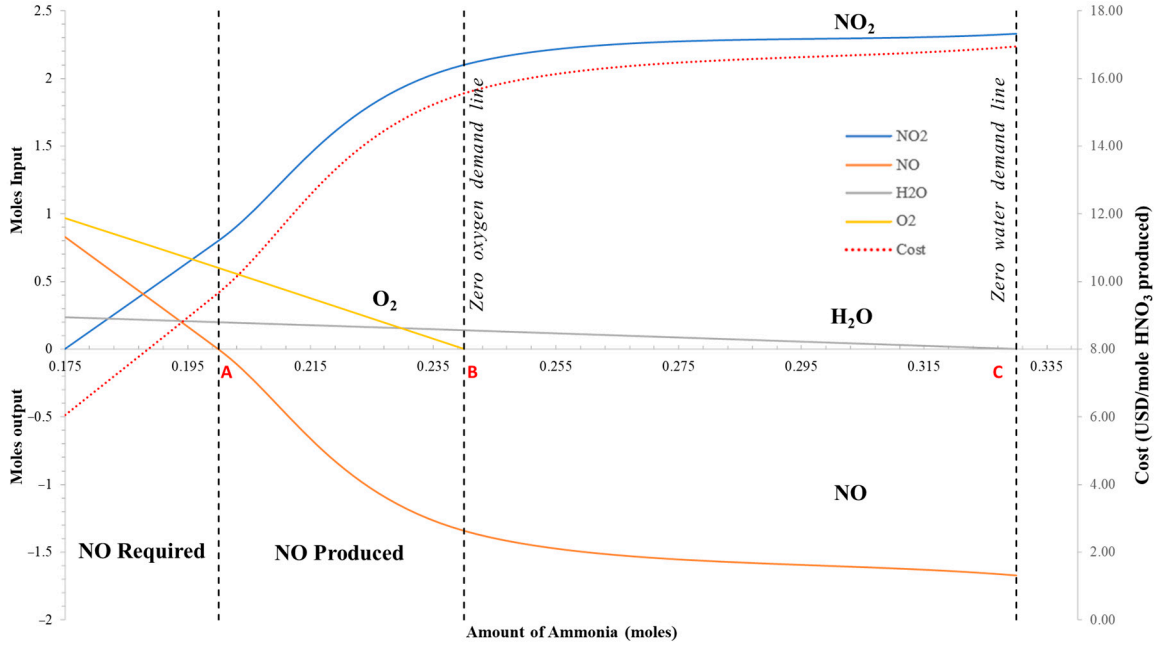

Figure 11. Molar amounts AR plot of each component required/produced as a function of the amount of ammonia fed to the process that produces one mole of nitric acid.

At point B, the O_2 demand of the process is reduced to zero, which allows one to achieve a zero oxygen-demand process. This is because O_2 in this region will be generated by the decomposition of NO_2. Conventionally, NH_3 is converted to NO and H_2O by catalytic oxidation with dry air [38]. This, however, requires an additional separation process to remove waste gases such as nitrogen, carbon dioxide, and a small number of other gases. With the possibility of an oxygen-free process, this additional separation process can be removed or modified to obtain a simpler downstream process.

Similarly, at point C, the water demand is reduced to 0, which could be used to synthesise a process with zero water demand. Water in the Ostwald process is mainly used for the absorption of concentrated NO_2 to form nitric acid [33]. If enough H_2O is produced from the oxidation of NH_3, the adsorption process will essentially become a self-sustaining process.

Additionally, incorporating a secondary plot of production cost could provide a better insight into the economics of the process. As seen in Figure 11, the overall cost of materials increases along with the demand for NO_2. This indicates that the recycling loop in the system could potentially reduce the overall cost of materials.

Similar practices can be implemented for changes in enthalpy and Gibbs energy. Figure 12 represents the overall changes in enthalpy and Gibbs energy as a function of ammonia fed to the process. In a process, a positive enthalpy means that the process is endothermic, an d heat addition is required to the process. On the other hand, a negative change of enthalpy in a process means that the process is exothermic, where heat will be released to the surroundings.

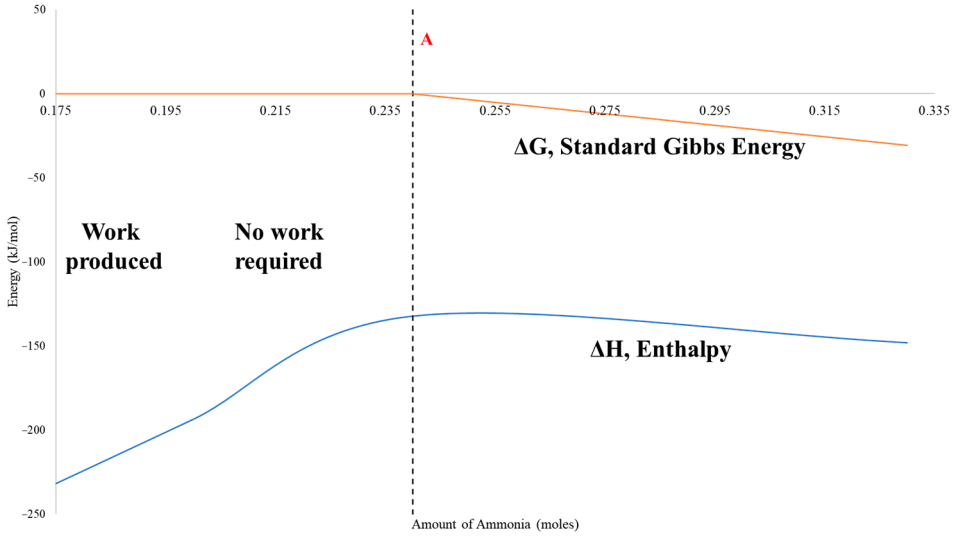

Figure 12. Gibbs energy and Enthalpy change AR plot for the Nitric acid synthesis process as a function of the ammonia fed to the process.

While interpreting in terms of Gibbs energy, a positive Gibbs energy shows that the process is non-spontaneous and work is required, while a negative Gibbs energy shows that the process is spontaneous and work is produced. In other terms, a positive Gibbs energy change indicates the process is not feasible, while a negative change indicates the process is feasible. Zero changes in Gibbs energy indicate an equilibrium process.

In the case of nitric acid synthesis, the enthalpy of the process decreases (more exothermic) as the Gibbs energy changes increase until the Gibbs energy changes reach zero. The enthalpy of the process then increases (less exothermic) as the ammonia feed increases while the Gibbs energy change is maintained at zero. The right side of line A indicates an equilibrium process that can be used as the process target.

Mathematical Validation of Results

The generated AR plot can be validated with a conventional mathematical method, which in this case is by solving the atomic balance equation. The mathematical method should produce similar results to the AR plot, as they both should correspond to each other. The process contains three atomic species, namely, nitrogen, hydrogen, and oxygen. Each of the species can be represented by Equations (11)–(13). The summation of all three atomic species equations will essentially yield Equation (5).

$$\text{Nitrogen} : a + d + e = 1 \tag{11}$$

$$\text{Oxygen} : 2a + 2b + c + d = 3 \tag{12}$$

$$\text{Hydrogen} : 2c + 3e = 1 \tag{13}$$

There are five variables and three atomic balance equations, therefore resulting in a DOF of two. Here, each of the components will be expressed in terms of ammonia and nitrogen dioxide, which correspond to the DOF. As shown in Table 3, H_2O can be expressed just in terms of ammonia with a linear equation. This is validated, as Figure 11 shows a straight line for the H_2O plot.

The equation shows that the H_2O requirement reaches zero at an ammonia feed rate of 0.333, which corresponds to the plotted AR graph. The other two components, O_2 and NO, are both expressed in terms of ammonia and NO_2. A system with two DOFs has a wide range of possible solutions. This problem, however, has been eliminated as the constraints in the P-graph generate only feasible answers. Identical results are found by substituting

the results from the P-graph into the dependency equation of O_2 and NO, which validates the accuracy of the AR plot.

Table 3. Dependency equation of each respective variable.

Variable	Component	Dependency Equation
b	O_2	$[O_2] = \frac{3-2[NO_2]+5[NH_3]}{4}$
c	H_2O	$[H_2O] = \frac{1-3[NH_3]}{2}$
d	NO	$[NO] = 1 - [NH_3] - [NO_2]$

Though the results prove that the AR plot corresponds to the P-graph solutions, there are still some limitations to this approach. The first limitation is that the DOF of the system affects the quality of the AR plot. A system with a high DOF means that there can be several solutions to a constant variable, which creates overlapping results. This problem can be improved by either reducing the DOF of the system, which can be achieved by reducing the number of reactants, or using an AR plot of higher dimensions. A three-dimensional AR plot can accommodate a system with a higher DOF and can provide even more insight into the problem.

Another limitation is that the results produced are solely based on theoretical constraints such as enthalpy and Gibbs energy and under the assumption of perfect process conversion. In reality, the rate and conversion of the actual process could be affected by many other factors, such as the efficiency of equipment and other conditions like pressure and temperature.

While estimating the cost of production, the purpose is to demonstrate the concept; thus, only the basic material is considered. This only provides a very basic insight into the economics of the system. Additionally, process configurations would also impact the economy of the system. The type and operating mode of equipment will define the capital and operating cost of the system. In order to attain a more precise estimation, a more detailed economic analysis can be performed on the solution based on the translated block diagram.

4. Conclusions

An extension of the PART methodology has been developed in this work. The main innovation is the generation of an AR plot to display P-graph solutions for easy interpretation by designers. Solution structures were produced based on materials and energy balance constraints. Each component is connected to a generation and consumption node that are interconnected by an element node to perform elemental balance. All the components are also connected to the enthalpy node to perform heat balance and the Gibbs node to perform work balance. The solution structure was produced using the ABB algorithm, and three out of five suitable solutions were selected for analysis. In order to provide a better understanding of the solution structure, each of the solution structures was translated into process block diagrams. An AR plot was constructed using the solution equation obtained from the P-graph based on the production of one mole of nitric acid. The plot provides meaningful insight into how the change in reactant affects the products. The results show the new potential configuration for a conventional process, such as those that involve a recycling loop. This expanded PART could be used as a new tool for a synthesis problem during the preliminary stage of a design process.

Future work can include using simulation software such as Aspen Plus v5.2.4.4 to simulate each solution structure. This allows a more in-depth understanding of the feasibility of each solution, as the current discussion is based solely on theoretical interpretation. Subsequently, more constraints such as reaction kinetics, reaction conditions, and catalysts can be considered to simulate a more precise solution. The capital and operating costs of each piece of equipment can also be considered for a more detailed economic analysis.

Author Contributions: Conceptualization, J.F.D.T.; Methodology, Y.S., V.W.G.T. and J.F.D.T.; Formal analysis, V.W.G.T.; Investigation, Y.S.; Writing—original draft, Y.S.; Writing—review & editing, R.R.T.; Project administration, D.C.Y.F. All authors have read and agreed to the published version of the manuscript.

Funding: This research received no external funding.

Data Availability Statement: Not Available.

Conflicts of Interest: The authors declare no conflict of interest.

References

1. Seider, W.D.; Widagdo, S.; Seader, J.D.; Lewin, D.R. Perspectives on chemical product and process design. *Comput. Chem. Eng.* **2009**, *33*, 930–935. [CrossRef]
2. Martín, M.; Adams, T.A., II. Challenges and future directions for process and product synthesis and design. *Comput. Chem. Eng.* **2019**, *128*, 421–436. [CrossRef]
3. Martin, M.; Gani, R.; Mujtaba, I.M. Sustainable process synthesis, design, and analysis: Challenges and opportunities. *Sustain. Prod. Consum.* **2022**, *30*, 686–705. [CrossRef]
4. Glavič, P.; Pintarič, Z.N.; Bogataj, M. Process Design and Sustainable Development—A European Perspective. *Processes* **2021**, *9*, 148. [CrossRef]
5. Douglas, J.M. A hierarchical decision procedure for process synthesis. *AIChE J.* **1985**, *31*, 353–362. [CrossRef]
6. Horn, F. Attainable and non-attainable regions in chemical reaction technique. In *Third European Symposium on Chemical Reaction Engineering*; Pergamon Press: London, UK, 1964; pp. 1–10.
7. Charis, G.; Danha, G.; Muzenda, E.; Glasser, D. Development trajectory of the attainable region optimization method: Trends and opportunities for applications in the waste-to-energy field. *S. Afr. J. Chem. Eng.* **2020**, *32*, 13–26. [CrossRef]
8. Patel, B.; Hildebrandt, D.; Glasser, D.; Hausberger, B. Synthesis and Integration of Chemical Processes from a Mass, Energy, and Entropy Perspective. *Ind. Eng. Chem. Res.* **2007**, *46*, 8756–8766. [CrossRef]
9. Mcgregor, C.; Hildebrandt, D.; Glasser, D. Process Synthesis for a Reactor-Separator-Recycle System using the Attainable Region Approach. *Dev. Chem. Eng. Miner. Process.* **1998**, *6*, 21–39. [CrossRef]
10. Hildebrandt, D.; Glasser, D.; Crowe, C.M. Geometry of the attainable region generated by reaction and mixing: With and without constraints. *Ind. Eng. Chem. Res.* **1990**, *29*, 49–58. [CrossRef]
11. Nicol, W.; Hernier, M.; Hildebrant, D.; Glasser, D. The attainable region and process synthesis: Reaction systems with external cooling and heating: The effect of relative cost of reactor volume to heat exchange area on the optimal process layout. *Chem. Eng. Sci.* **2001**, *56*, 173–191. [CrossRef]
12. Moodley, A.; Kauchali, S.; Hildebrandt, D.; Glasser, D. Debottlenecking the Ammonia Synthesis Reactor System with the Aid of Attainable Region Theory. In Proceedings of the AIChE Annual Meeting, Conference Proceedings, Austin, TX, USA, 7–12 November 2004; American Institute of Chemical Engineers: New York, NY, USA, 2004; pp. 5677–5687.
13. Tran, T.T.A.; Le, T.K.P.; Mai, T.P.; Nguyen, D.Q. Bioethanol Production from Lignocellulosic Biomass. In *Alcohol Fuels-current Technologies and Future Prospect*; Yun, Y., Ed.; IntechOpen: London, UK, 2019; Chapter 4. [CrossRef]
14. Scott, F.; Conejeros, R.; Aroca, G. Attainable region analysis for continuous production of second generation bioethanol. *Biotechnol. Biofuels* **2013**, *6*, 171. [CrossRef] [PubMed]
15. Friedler, F.; Orosz, Á.; Losada, J.P. *P-Graphs for Process Systems Engineering*; Springer: Berlin/Heidelberg, Germany, 2022.
16. Friedler, F.; Aviso, K.B.; Bertok, B.; Foo, D.C.Y.; Tan, R.R. Prospects and challenges for chemical process synthesis with P-graph. *Curr. Opin. Chem. Eng.* **2019**, *26*, 58–64. [CrossRef]
17. Friedler, F.; Tarján, K.; Huang, Y.W.; Fan, L.T. Graph-theoretic approach to process synthesis: Axioms and theorems. *Chem. Eng. Sci.* **1992**, *47*, 1973–1988. [CrossRef]
18. Friedler, F.; Tarjan, K.; Huang, Y.W.; Fan, L.T. Combinatorial algorithms for process synthesis. *Comput. Chem. Eng.* **1992**, *16*, S313–S320. [CrossRef]
19. Friedler, F.; Varga, J.B.; Fehér, E.; Fan, L.T. Combinatorially Accelerated Branch-and-Bound Method for Solving the MIP Model of Process Network Synthesis. In *State of the Art in Global Optimization: Computational Methods and Applications*; Floudas, C.A., Pardalos, P.M., Eds.; Springer: Berlin/Heidelberg, Germany, 1996; pp. 609–626. [CrossRef]
20. P-Graph. 2023. Available online: http://p-graph.com/ (accessed on 12 July 2023).
21. Varbanov, P.; Friedler, F.; Klemeš, J. Process Network Design and Optimisation Using P-graph: The Success, the Challenges and Potential Roadmap. *Chem. Eng. Trans.* **2017**, *61*, 1549–1554. [CrossRef]
22. Liu, J.; Fan, L.T.; Seib, P.; Friedler, F.; Bertok, B. Downstream process synthesis for biochemical production of butanol, ethanol, and acetone from grains: Generation of optimal and near-optimal flowsheets with conventional operating units. *Biotechnol. Prog.* **2004**, *20*, 1518–1527. [CrossRef]
23. Tan, R.R.; Aviso, K.B.; Foo, D.C.Y. P-graph and monte carlo simulation approach to planning carbon management networks. *Comput. Chem. Eng.* **2017**, *106*, 872–882. [CrossRef]

24. Chong, F.K.; Lawrence, K.K.; Lim, P.P.; Poon, M.C.Y.; Foo, D.C.Y.; Lam, H.L.; Tan, R.R. Planning of carbon capture storage (ccs) deployment using P-graph approach. *Energy* **2014**, *76*, 641–651. [CrossRef]
25. Lim, C.H.; Pereira, P.S.; Shum, C.K.; Ong, W.J.; Tan, R.R.; Lam, H.L.; Foo, D.C.Y. Synthesis of resource conservation networks with p-graph approach—Direct reuse/recycle. *Process Integr. Optim. Sustain.* **2017**, *1*, 69–86. [CrossRef]
26. Seo, H.; Lee, D.Y.; Park, S.; Fan, L.T.; Shafie, S.; Bertók, B.; Friedler, F. Graph-theoretical identification of pathways for biochemical reactions. *Biotechnol. Lett.* **2001**, *23*, 1551–1557. [CrossRef]
27. Fan, L.T.; Bertók, B.; Friedler, F. A graph-theoretic method to identify candidate mechanisms for deriving the rate law of a catalytic reaction. *Comput. Chem.* **2002**, *26*, 265–292. [CrossRef] [PubMed]
28. Lakner, R.; Bertók, B.; Friedler, F. Synthesis of startable reaction pathways. *Chem. Eng. Trans.* **2018**, *70*, 1129–1134.
29. Bertok, B.; Heckl, I. Chapter Nine—Process Synthesis by the P-Graph Framework Involving Sustainability. In *Synthesis and Analysis of Chemical Engineering Processes*; Ruiz-Mercado, G., Cabezas, H., Eds.; Springer: Berlin/Heidelberg, Germany, 2016; pp. 203–225. [CrossRef]
30. Pimentel, J.; Orosz, Á.; Aviso, K.B.; Tan, R.R.; Friedler, F. Conceptual Design of a Negative Emissions Polygeneration Plant for Multiperiod Operations Using P-Graph. *Processes* **2021**, *9*, 233. [CrossRef]
31. Tapia, J.F.D.; Evangelista, D.G.; Aviso, K.B.; Tan, R.R. P-graph Attainable Region Technique (PART) for Process Synthesis. *Chem. Eng. Trans.* **2022**, *94*, 1159–1164. [CrossRef]
32. Cheremisinoff, P.N. Chapter 7—Industry Profile—Fertilizers. In *Waste Minimization and Cost Reduction for the Process Industries*; Cheremisinoff, P.N., Ed.; William Andrew Publishing: Norwich, NY, USA, 1995; pp. 222–284. [CrossRef]
33. Rouwenhorst, K.H.R.; Jardali, F.; Bogaerts, A.; Lefferts, L. From the Birkeland-Eyde process towards energy-efficient plasma-based NOX synthesis: A techno-economic analysis. *Energy Environ. Sci.* **2021**, *14*, 2520–2534. [CrossRef]
34. Chase, M. *NIST-JANAF Thermochemical Tables*, 4th ed.; American Institute of Physics: College Park, MD, USA, 1998.
35. Franck, E.U.; Cox, J.D.; Wagman, D.D.; Medvedev, V.A. CODATA—Key Values for Thermodynamics, aus der Reihe: CODATA, Series on Thermodynamic Properties. Hemisphere Publishing Corporation, New York, Washington, Philadelphia, London 1989. 271 Seiten, Preis: £ 28.00. *Berichte Bunsenges. Phys. Chem.* **1990**, *94*, 93. [CrossRef]
36. Friedler, F.; Tarjan, K.; Huang, Y.W.; Fan, L.T. Graph-theoretic approach to process synthesis: Polynomial algorithm for maximal structure generation. *Comput. Chem. Eng.* **1993**, *17*, 929–942. [CrossRef]
37. Friedler, F.; Orosz, Á.; Pimentel Losada, J. Accelerated Branch-and-Bound Algorithm of Process Network Synthesis. In *P-graphs for Process Systems Engineering: Mathematical Models and Algorithms*; Friedler, F., Orosz, Á., Pimentel Losada, J., Eds.; Springer International Publishing: Berlin/Heidelberg, Germany, 2022; pp. 63–81. [CrossRef]
38. Laan, P.C.M.; Franke, M.C.; van Lent, R.; Juurlink, L.B.F. Heterogeneous Catalytic Oxidation of Ammonia by Various Transition Metals. *J. Chem. Educ.* **2019**, *96*, 2266–2270. [CrossRef]